Impact of Insulation and Cooling on Performance due to Reliability-Oriented Design of Electrical Machines

Lucas Vincent Hanisch, Jonas Franzki, Markus Henke
Institute for Electrical Machines, Traction and Drives, TU Braunschweig
Hans-Sommer-Straße 66
Braunschweig, Germany
Phone: +49 (0) 531-3913906
Email: l-v.hanisch@tu-braunschweig.de
URL: http://www.tu-braunschweig.de/imab

Keywords

≪Permanent magnet motor≫, ≪Insulation≫, ≪Thermal model≫, ≪Cooling≫, ≪Reliability≫

Abstract

In this paper, a multiphysics model of a permanent magnet synchronous motor (PMSM) is created to investigate the influence of the cooling and insulation system on the temperature distribution and performance of the machine. In thermal computer fluid dynamic (CFD) studies, the influence of the coolant flow, the winding head impregnation and the insulation paper on the temperature distribution of the machine is investigated. Finally, the influence of thermal effects on the steady-state limit torque of the machine is evaluated. It is systematically shown that insulation materials with high thermal conductance allow torque increases of about 3.3%. Torque can be increased by about 1.9% per reduced 0.1 mm insulation thickness of the slot liner. Alternatively, the temperature impact on insulation can be reduced at constant torque leading to improved insulation lifetime and reliability.

Introduction

Increasing power densities of electrical machines for advanced applications in electromobility lead to an intensified focus on the electrical insulation system as a critical component. The reason for this is that with increased voltage and power density, the percentage of insulation failures in the stator winding of electrical machines has increased from 36% to 66% [1]. The damage of insulation is the consequence of erosion processes that accelerate with increased temperature and lead to winding short circuits [2]. To prevent these damage mechanisms and to take them into account in the design of electrical machines, an early focus on insulation stresses and reliability leading to a reliability-oriented design is becoming increasingly important [3].

Therefore, many studies investigate the lifetime and reliability of windings and insulation systems as a function of temperature. In [4], the partial discharge inception voltage is used to assess the condition of enamel-insulated copper wires and their behavior under different thermal boundary conditions is investigated. In [5], similar results were obtained for slot liners.

The objective of the research presented in this paper is to investigate the thermal effects and interactions of different insulation systems and cooling mechanisms, and to determine the impact on machine performance.

For this purpose, a PMSM is investigated with a multiphysics model. Since the power loss calculation is very important for the thermal investigations, it is evaluated in more detail in 2D and 3D simulations. In the thermal analysis, the slot is homogenized according to [6] and modeled as a composite of conductor,

insulating varnish, and impregnating resin. This model is analyzed in CFD studies to evaluate different thermal effects on steady state performance.

Electromagnetic modeling of the PMSM

In this chapter, the electrical modeling of the PMSM is explained. The correct meshing of the model is explicitly discussed in order to be able to perform precise loss calculations in an acceptable time and reduce numerical noise [7].

Comparison of 2D and 3D model

When calculating losses from 2D models, one should consider that end effects such as leakage fluxes at the axial ends of the machine are neglected and that iron and magnetic losses tend to be underestimated [7]. For the machine under consideration, the 2D and 3D meshes including the data on the meshes can be seen in Fig. 1 and Table I. The 3D meshing has 1.19 million elements, almost 17 times as many as the 2D meshing. The 3D mesh resolution was limited by time and RAM resources. Edge length and time step were chosen in a way that a harmonic stepping according to the circumferential speed was achieved. Table I shows, that in 2D simulation a much higher resolution can be achieved at lower computation time.

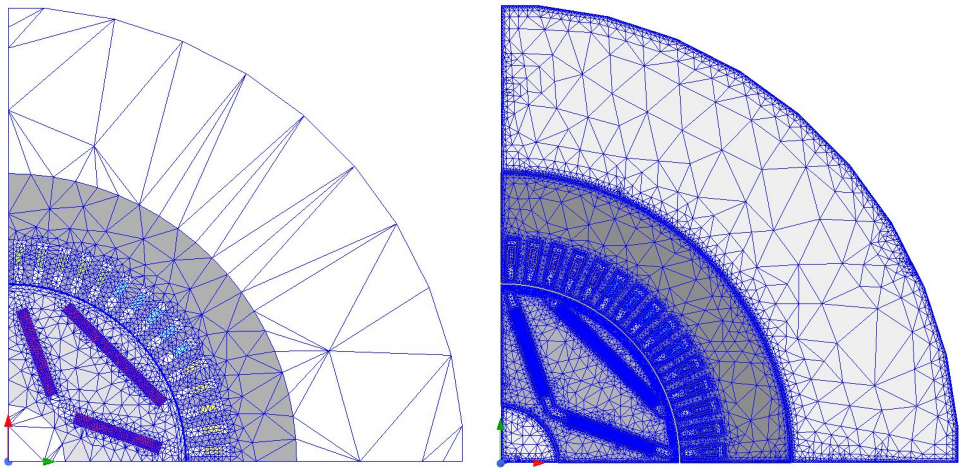

(a) **(b)**

Fig. 1: Comparison of 3D mesh (a) and 2D mesh (b)

Table I: Quantitative comparison of the two meshes

Attribute	Value
3D simulation	
Number of circumferential segments	180
Time step	16.667 µs
Max. edge length - surfaces	2.72969495 mm
Max. edge length - magnets	1.5 mm
Element number	1.19 Mio.
2D simulation	
Number of circumferential segments	600
Time step	10 µs
Max. edge length	0.40945424251787 mm
Element number	70,823

Loss calculation

Fig. 2a and Fig. 2b show the results of loss calculations at 220 Nm and 5000 rpm. It confirms the result of [8] that the power losses calculated by the simulation settle only after the first electrical period (6 ms). Up to this point, especially the hysteresis losses have not yet reached a steady state, but double from 3 to 6 ms. It is therefore reasonable to use the power losses from 6 ms for the evaluation.

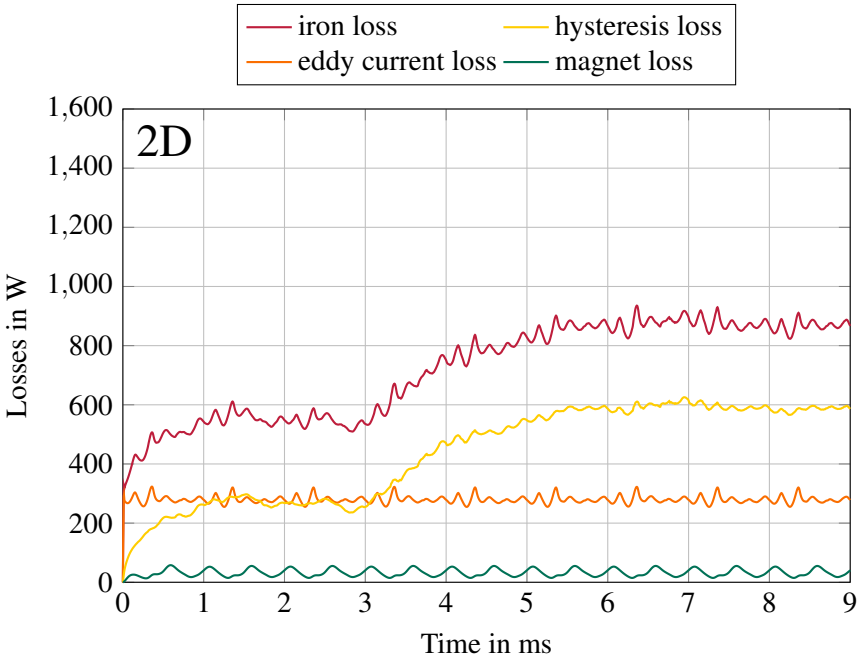

(a) 2D simulation

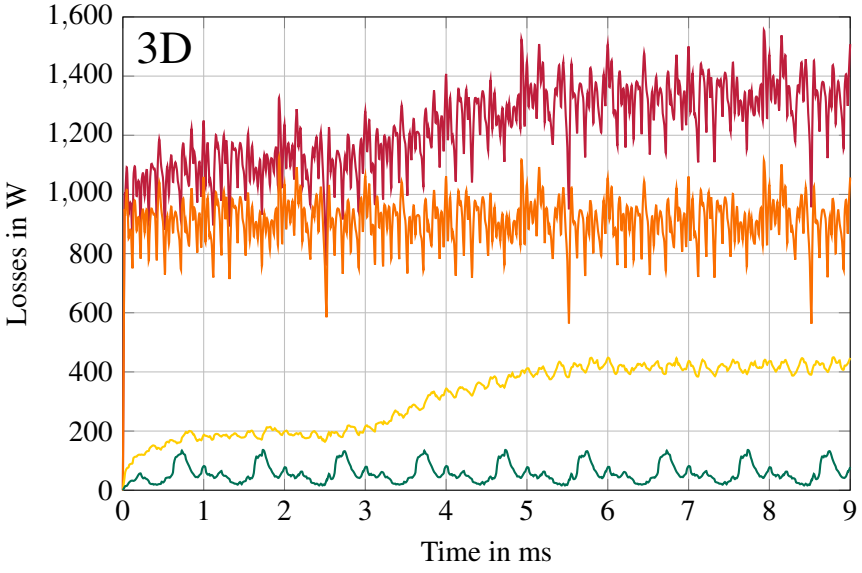

(b) 3D simulation

Fig. 2: Losses plotted against simulation time, M = 220 Nm, n = 5000 rpm

Beyond the plots, there are also significant differences between the 3D and 2D simulations. For example, in the 3D simulation, the eddy current losses reach significantly higher values than the hysteresis losses, whereas this is observed in reverse in the 2D simulation. Moreover, in the 3D simulation, the eddy current and iron losses are subject to high noise.

The losses of the 2D simulation are only higher than those of the 3D simulation in the case of hysteresis losses. On average, the losses calculated via 2D simulation are about 20% lower than those of the 3D

simulation. The difference could be caused by the consideration of the third dimension, which is pointed out in particular by Lundmark et al. in [7]. However, they also show that too low temporal and spatial resolution can strongly distort the results. This is suspected due to the discussed strong noise behavior in 3D simulation. They additionally point out that for a very high resolution of the 2D simulation, a better match with a high resolution 3D simulation can be achieved. The resolution of the 2D simulation with 1,200 time steps per revolution is already at a very high level [7]. For the reasons listed, from now on the 2D simulation results will be used for the thermal calculations.

Thermal modeling

To investigate dynamic aspects, the first step is to analyse the continuous operation of the electric machine at the nominal point (current density of 8 A/mm^2 for 220 Nm at 5,000 rpm). Electromagnetically, it can be assumed that the power losses are constant in time. This is permissible because the thermal time constant is much larger than the electromagnetic one. A meander cooling jacket is used for the simulated machine and shown in Fig. 3. The loops are implemented in such a way that a cooling channel runs axially every 30° and is connected to the next axial cooling channel by a meander loop above each winding head. In this way, one axial channel cools five slots and the circumference can be reduced to just these five slots. When choosing a meander cooling jacket, a challenge remains: Per meander, the coolant also heats up, so that in the last meander the coolant is warmer than in the first. This is accompanied by a lower temperature difference to the stator in the last meander and thus also a poorer cooling effect. This can be taken into account by either

- a meander loop is solved and the fluid dynamic and thermal results of the output are defined as a new input, so that step by step all meander loops are solved and the full representation of the machine is created, or
- the engine is not thermally modeled and consequently only the power loss is directly impressed on the cooling jacket, or
- an increased input temperature of the coolant for the individual meander loop is assumed, so that approximately the average cooling temperature of the fluid is reflected, whereby a certain result blurring is accepted

so that a circumferential reduction is still possible.

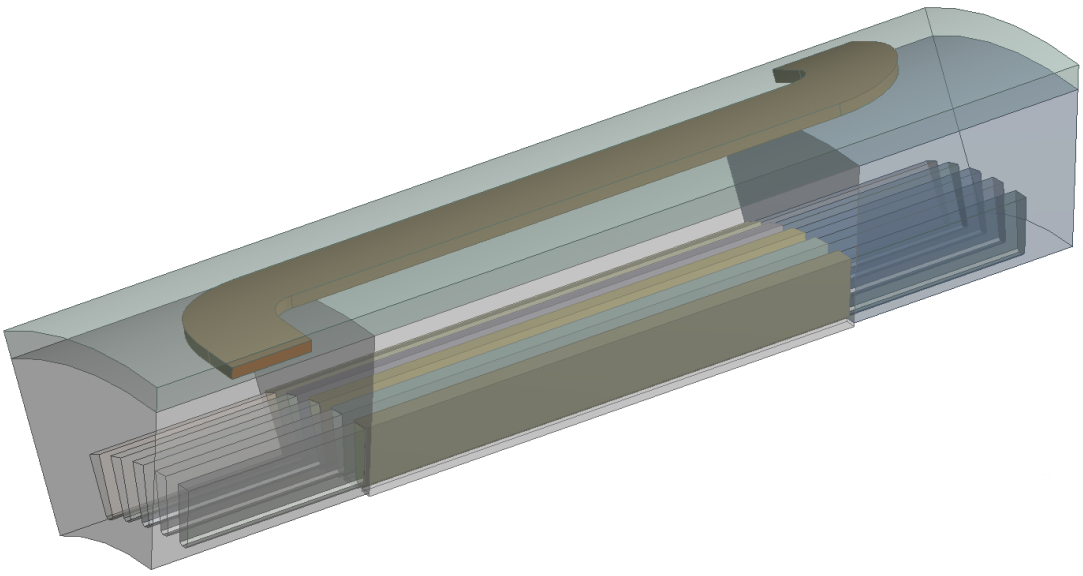

Fig. 3: Modeled section of the stator with meander-shaped cooling jacket

Investigation of thermal effects and insulation

The influence of the coolant flow on the temperature is to be investigated first. Fig. 4 shows on the left the maximum temperature of different machine components above the coolant flow for two operating points with current densities of 14 A/mm^2 (T_{max} = 180°C are reached) and 8 A/mm^2. It can be seen that, especially in the range below 3 l/min, an increase in flow rate can still reduce the temperature considerably. Above 6 l/min, the temperatures are hardly lowered. An exclusive consideration of the volume flow is not sufficient for an assessment of the quality of the cooling system, because it only describes the benefit achieved by a higher flow velocity, but not the required effort. To take the effort into account, the Stanton number is used as a quality criterion. This puts the heat transfer in relation to the required flow. In Fig. 4, it can be seen on the right that the Stanton number drops for increasing coolant flows, especially above 6 l/min. It can be seen that increasing the coolant flow increases the heat transfer coefficient, but the velocity of the fluid increases to a greater extent.

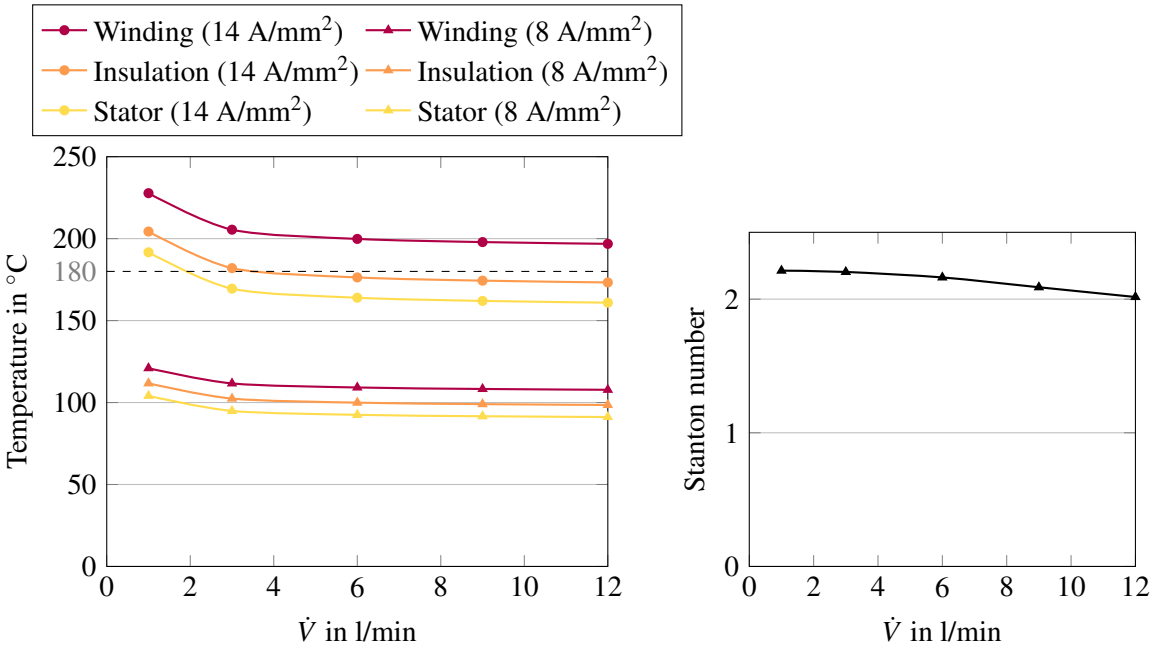

(a) Maximum temperatures

(b) Stanton number

Fig. 4: Maximum temperatures and Stanton number plotted against coolant flow rate

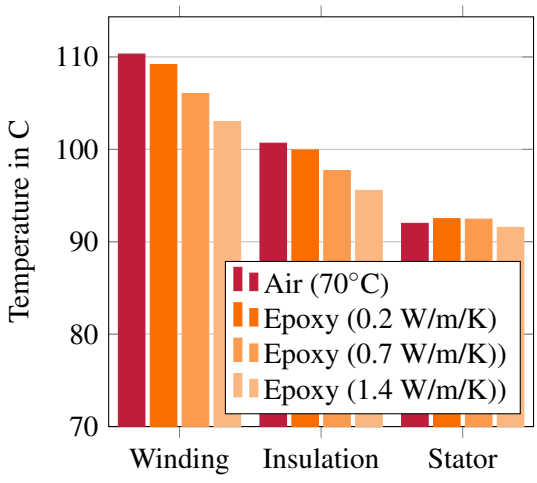

Fig. 5: Maximum temperatures for different potting materials

In addition to cooling, the influence of the insulation system on the thermal performance of the machine is investigated. For this purpose, Fig. 5 evaluates the temperature with different epoxy-based insulating resins. The results show that an epoxy impregnation causes a temperature reduction in the winding and insulation compared with air, irrespective of the thermal conductivity. On the stator, the epoxy impregnation initially has a temperature-increasing effect, since an additional heat input is formed from the winding head via the epoxy into the stator. Depending on the thermal conductivity, epoxy impregnation can reduce the temperature in the slot insulation by up to 5 degrees. In addition to the electrical properties studied here, thermally optimized insulation resins may differ in mechanical or chemical prop-

erties. This must be taken into account in the processing of the insulation resins, which may result in the revision of manufacturing steps.

Finally, the thickness of the slot liner was varied and the effects on temperature were studied. In Fig. 6, a linear relationship between temperature and insulation thickness can be observed. This observation is consistent with equation for heat transfer ($\Delta T = -\frac{\dot{Q}}{A\lambda}\delta$), which states that the temperature difference ΔT increases linearly with insulation thickness δ. The average slope - i.e. the temperature increase that occurs per layer increase of the insulation by 0.1 mm - for the maximum temperature is approx. $1,44\ \frac{\mathrm{K}}{0{,}1\ \mathrm{mm}}$ for the winding and at $1,52\ \frac{\mathrm{K}}{0{,}1\ \mathrm{mm}}$ for the insulation. The average temperature of the insulation shows a lower dependence on the layer thickness ($0,75\ \frac{\mathrm{K}}{0{,}1\ \mathrm{mm}}$). The temperature of the stator remains almost unaffected.

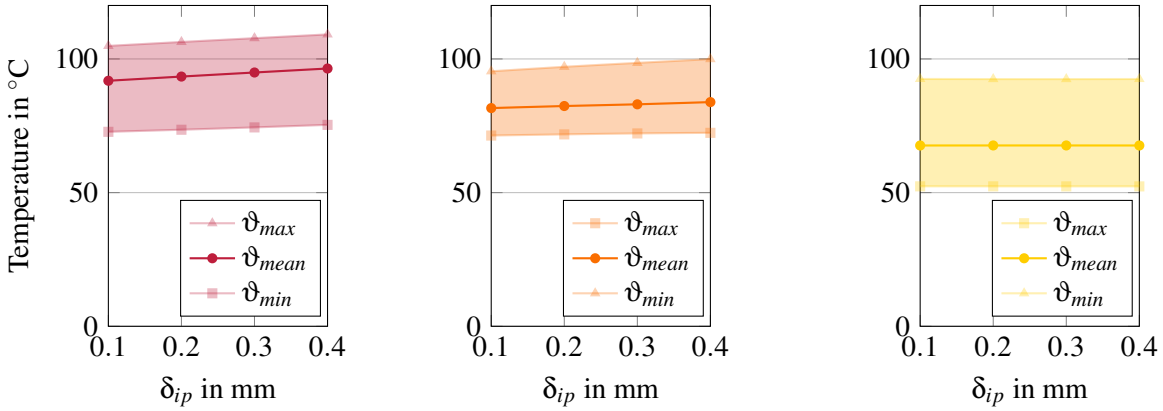

(a) Winding **(b)** Insulation **(c)** Stator

Fig. 6: Temperatures plotted against the thickness of the insulation paper δ_{ip}

Influences on the limit torque of the PMSM

Finally, the influence of the slot liner on the torque density of the PMSM is investigated. For this purpose, on the one hand the layer thickness of the slot liner is reduced from 0.4mm to 0.1mm. On the other hand, two different slot liners with a thermal conductivity of 0.2 W/mK (IP1) and 0.38 W/mK (IP2) are compared.

The evaluation of Table II shows that a slot liner 2 with higher thermal conductivity already results in a torque increase of 3.3% at the same thickness compared to slot liner 1 with 0.4 mm thickness. Reducing the layer thickness by 75% to 0.1 mm would result in a torque increase of 5.8%, i.e. a torque increase of about 1.9% per 0.1 mm reduction in insulation thickness. A combination of both measures (higher conductivity and 25% thickness) would finally result in a maximum torque increase of 7.6%. It should be noted that the performance increase due to thinner insulation papers is opposed by a reduced robustness against electrical breakdown and partial discharge. In addition, high thermal conductive insulation papers are more expensive than ordinary insulation papers and are therefore avoided in applications with increased focus on costs.

Table II: Results of investigated torque/IP dependency

Insulation material (thickness)	Current density A/mm²	Torque Nm	Torque increase Nm	Torque increase %
IP1 (0,4 mm)	14,2	428	–	–
IP2 (0,4 mm)	14,6	442	14	3,3
IP1 (0,1 mm)	14,9	453	25	5,8
IP2 (0,1 mm)	15,1	460	32	7,6

Conclusion and Outlook

It was shown that an increased coolant flow significantly reduces the temperature of the PMSM only up to a certain volume flow and that the increased cooling effort can be taken into account with the Stanton number. The temperature reduction in the winding and insulation as a result of different epoxy resins and the layer thickness of the slot liner was shown. This can be exploited in a reliability-oriented machine design, so that either the performance of the machine can be increased with the same geometry, or the machine dimensions can be reduced while maintaining the same reliability. However, this also increases cost and weight, which is why it should be subject to a trade-off analysis. At the maximum, the heat dissipation of the PMSM could be optimized by using a more conductive and thinner insulation paper to such an extent that a higher current density enables a torque increase of 7.6% at the same temperature.

In future investigations, the simulation results are to be verified on reference machines or motorettes with different insulation materials. In addition to investigations of the thermal characteristics or torque of the electrical machine, the reliability of the various insulation systems can be assessed by partial discharge measurements.

References

[1] J. He, C. Somogyi, A. Strandt and N. A. O. Demerdash, "Diagnosis of stator winding short-circuit faults in an interior permanent magnet synchronous machine," 2014 IEEE Energy Conversion Congress and Exposition (ECCE), 2014, pp. 3125-3130, doi: 10.1109/ECCE.2014.6953825.

[2] Pietrzak P, Wolkiewicz M. Comparison of Selected Methods for the Stator Winding Condition Monitoring of a PMSM Using the Stator Phase Currents. Energies. 2021; 14(6):1630. https://doi.org/10.3390/en14061630

[3] M. Galea, P. Giangrande, V. Madonna and G. Buticchi, "Reliability-Oriented Design of Electrical Machines: The Design Process for Machines' Insulation Systems MUST Evolve," in IEEE Industrial Electronics Magazine, vol. 14, no. 1, pp. 20-28, March 2020, doi: 10.1109/MIE.2019.2947688.

[4] F. Pauli, N. Driendl and K. Hameyer, "Study on Temperature Dependence of Partial Discharge in Low Voltage Traction Drives," 2019 IEEE Workshop on Electrical Machines Design, Control and Diagnosis (WEMDCD), 2019, pp. 209-214, doi: 10.1109/WEMDCD.2019.8887790.

[5] K. Bae et al., "Current State and Development Trends of Insulation Systems in BEV Traction Motors Steered by Electric Powertrain Innovation," PCIM Europe digital days 2021; International Exhibition and Conference for Power Electronics, Intelligent Motion, Renewable Energy and Energy Management, 2021, pp. 1-8.

[6] L. Idoughi, X. Mininger, F. Bouillault, L. Bernard and E. Hoang, "Thermal Model With Winding Homogenization and FIT Discretization for Stator Slot," in IEEE Transactions on Magnetics, vol. 47, no. 12, pp. 4822-4826, Dec. 2011, doi: 10.1109/TMAG.2011.2159013.

[7] S. T. Lundmark and P. R. Fard, "Two-Dimensional and Three-Dimensional Core and Magnet Loss Modeling in a Radial Flux and a Transverse Flux PM Traction Motor," in IEEE Transactions on Industry Applications, vol. 53, no. 3, pp. 2028-2039, May-June 2017, doi: 10.1109/TIA.2017.2671416.

[8] S. T. Lundmark, A. Acquaviva and A. Bergqvist, "Coupled 3-D Thermal and Electromagnetic Modelling of a Liquid-cooled Transverse Flux Traction Motor," 2018 XIII International Conference on Electrical Machines (ICEM), 2018, pp. 2640-2646, doi: 10.1109/ICELMACH.2018.8506835.